S. Vantieghem · X. Albets-Chico ·
B. Knaepen

The velocity profile of laminar MHD flows in circular conducting pipes

Abstract We present numerical simulations without modeling of an incompressible, laminar, unidirectional circular pipe flow of an electrically conducting fluid under the influence of a uniform transverse magnetic field. Our computations are performed using a finite-volume code that uses a charge-conserving formulation (called current-conservative formulation in references [12] and [13]). Using high resolution unstructured meshes, we consider Hartmann numbers up to 3000 and various values of the wall conductance ratio c. In the limit $c \ll Ha^{-1}$ (insulating wall), our results are in excellent agreement with the so-called asymptotic solution [1]. For higher values of the wall conductance ratio, a discrepancy with the asymptotic solution is observed and we exhibit regions of velocity overspeeds in the Roberts layers. We characterize these overspeed regions as a function of the wall conductance ratio and the Hartmann number; a set of scaling laws is derived that is coherent with existing asymptotic analysis.

Keywords MHD, Numerics, Circular pipe, Wall-conductivity

1 Introduction

Magnetic fields can influence the flow of electrically conducting fluids, and are therefore of important theoretical and practical interest. Applications that concern liquid metals or electrolytes are, among others, the damping of turbulence in casting processes, the flow of lithium in the breeder blankets of future fusion devices, or electromagnetic flow meters that allow to measure flow rates in a non-intrusive way. One of the most basic problems that can be considered, is the determination of the laminar flow profile in a

Physique statistique et des plasmas (PSP), Faculté des Sciences, Université Libre de Bruxelles (ULB) Campus de la Plaine, CP231, Bvd. du Triomphe, 1050 Bruxelles, Belgium. E-mail: stvtiegh@ulb.ac.be.

circular pipe under a uniform magnetic field, i.e. the magnetohydrodynamic variant of Poiseuille pipe flow. Pioneering theoretical and experimental works for this geometry were done by Hartmann and Lazarus [2], [3]. In the 60's, analytical solutions were obtained for pipes with insulating [4] as well as conducting walls [5]. A later analytical work by Samad [6] considered the case of a pipe with finite wall thickness and observed overspeed regions in the velocity profile of the MHD pipe flow. However, all these solutions are under the form of infinite series expansions involving modified Bessel functions, which make them difficult to evaluate, certainly when the intensity of the Lorentz forces compared to viscous forces, as expressed by Hartmann number (Ha), is high. This era saw also the birth of various approximative solutions, based on asymptotic methods [1], [7], [8]. The results obtained through the asymptotic methods, tend to become better as the Hartmann number increases, but it was also pointed out that the approximate solutions provided, break down near to where the wall is parallel to the magnetic field. At that point in history, the problem of the laminar pipe flow under a uniform magnetic field, was considered to be more or less solved and attention was directed to more challenging flows in complex geometries, magnetic field configurations or in turbulent regimes, also favoured by the exponential increase in computing power and the development of CFD tools, although the simulation of high Hartmann number flows in finite-difference or finite-volume codes remained to suffer from large numerical errors [9].

In this work, we revisit the basic problem of circular pipe flow under the influence of a uniform magnetic field by means of high resolution numerical simulations based on the finite-volume method. Given recent progress in the numerical algorithms available to compute MHD flows, one can now reach much higher Hartmann numbers without the need of specific modeling. This allows us to compute accurately the laminar velocity profile of the flow and confirm the presence of "jets" in the Roberts layers, as first reported in [6]. However, by considering high values of the Hartmann number, we show that the intensity of these "jets" is $O(Ha^0)$ (and not $O(Ha^{1/2})$ like the velocity profiles in rectangular ducts with walls of finite conductivity or $O(Ha)$ in Hunt's flow) so we refer to them as overspeed regions. We also provide a set of scaling laws that is coherent with existing asymptotic analyses.

2 Mathematical formulation

We consider the incompressible, unidirectional flow $\mathbf{u} = u(x, y)\mathbf{1_z}$ of an electrically conducting fluid through a circular pipe of radius L and of infinite extent in the axial direction (see figure 1). The fluid can be characterized by its density ρ, kinematic viscosity ν and conductivity σ. An external magnetic field $\mathbf{B} = B_0\mathbf{1_y}$ is imposed. The flow is driven by a uniform pressure gradient in the axial direction, $-\nabla p = f\mathbf{1_z}$. We assume that the magnetic Reynolds number $R_m = \mu\sigma UL$ (with U a typical velocity scale and μ the magnetic permeability) is much smaller than one, so that the induced magnetic field is negligible compared to the applied one, and that we can invoke the quasistatic approximation [10]. To obtain non-dimensional equations, we rescale the variables as follows: $\mathbf{u} \to U\,\mathbf{u}$, $\mathbf{B} \to B_0\,\mathbf{1_y}$, $\nabla \to L^{-1}\,\nabla$, $t \to \rho/(\sigma B_0^2)t$,

$\mathbf{j} \rightarrow \sigma U B_0 \mathbf{j}$, $\phi \rightarrow U B_0 L \phi$ and $p \rightarrow \sigma U L B_0^2 p$, with $U = f/(\sigma B_0^2)$. The steady, uni-directional, flow profile can then be found from the following two conservation laws:

$$\partial_t \mathbf{u} = Ha^{-2}\nabla^2\mathbf{u} + \mathbf{j} \times \mathbf{1_y} + \mathbf{1_z} = 0 \tag{1}$$

$$\nabla \cdot \mathbf{j} = \nabla \cdot (-\nabla\phi + \mathbf{u} \times \mathbf{1_y}) = 0 \tag{2}$$

The first equation is a simplified version of the incompressible Navier-Stokes equations for steady flows, where the nonlinear term does not appear because of the unidimensional character of the flow, and where the Lorentz force term is added. The only free parameter is the aforementioned Hartmann number Ha; it is a measure of the square root of the ratio between electromagnetic and viscous forces:

$$Ha = B_0 L \sqrt{\frac{\sigma}{\rho\nu}} \tag{3}$$

The second equation expresses the conservation of charge, where Ohm's law for a moving fluid has been inserted. It is a Poisson type equation for the electrical potential:

$$\nabla^2\phi = \nabla \cdot (\mathbf{u} \times \mathbf{1_y}) \tag{4}$$

Suitable boundary conditions still need to be imposed in order to close the problem. For the velocity field, we use the no-slip condition $u|_{wall} = 0$. The boundary condition for the potential is more intricate. In fact, we could solve the Poisson equation (4) in a combined fluid-wall domain, with insulating conditions at the outer wall boundary and impose continuity at the wall-fluid interface. However, when the thickness of the wall is small compared to the pipe radius, we can us the so-called thin wall approximation [11], which assumes that currents discharge tangentially in the wall. This condition reads:

$$\partial_n\phi = \nabla_\tau \cdot (c\nabla_\tau\phi) \tag{5}$$

where ∇_τ stands for the component of the ∇-operator tangential to the wall and $\partial_n = \mathbf{n} \cdot \nabla$ with $\mathbf{n}$ the outward pointing normal vector on the wall (see figure 1). At last, c is the so called wall-conductance ratio defined as:

$$c = \frac{\sigma_w d_w}{\sigma L} \tag{6}$$

with σ_w and d_w the wall conductivity and thickness. It is easily seen that in the limit of perfectly conducting (insulating) walls, we recover the familiar Dirichlet (Neumann) condition.

3 Phenomenology

In figure 1, the basic features of the MHD pipe flow are represented. In the limit of high Hartmann numbers, three distinct regions can be considered: the core of the flow, the Hartmann layers and the Roberts layers [1,7].

In the core region, the velocity profile is approximately flat in the direction of the magnetic field and the current density generated is uniform $\mathbf{j} \sim \mathbf{u} \times \mathbf{1_y}$;
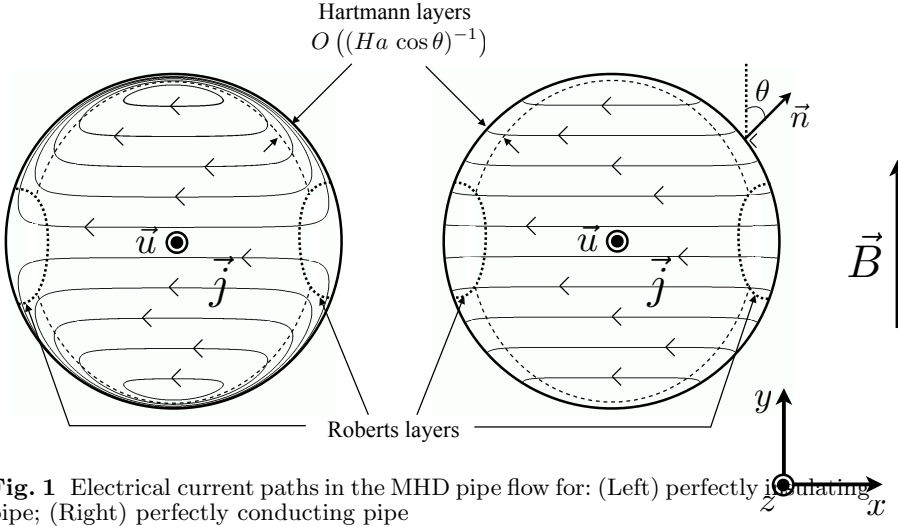
Fig. 1 Electrical current paths in the MHD pipe flow for: (Left) perfectly insulating pipe; (Right) perfectly conducting pipe

the momentum balance is governed by the imposed pressure gradient and the Lorentz force since viscous effects are negligible. Since the current lines must form closed paths in the combined pipe-wall domain, a potential is induced that changes the direction of the currents in viscous boundary layers and drives them along the wall and/or makes them enter into the wall, depending on the wall conductance ratio.

The Hartmann layers are located in the vicinity of the pipe's wall, where its normal vector is not perpendicular the magnetic field. In the Hartmann layers, the momentum balance is largely dominated by the Lorentz force and viscous effects. This gives rise to an exponential drop-off in the velocity profile as one approaches the wall.

Finally, the Roberts layers are defined as the regions in the pipe's cross section that are adjacent to its wall, and where the normal vector to the wall is perpendicular the magnetic field. In the Roberts layers, the velocity profile is determined by the combined balance between the pressure gradient, the Lorentz force and the viscous effects. As the Hartmann number increases, the extent of the Roberts layers decreases as well as their contribution to the total mass flow in the pipe. An a priori prediction of the velocity profile in the Roberts layers is very difficult since it depends in a subtle way on the exact direction of the electric currents in these viscous boundary layers.

In the traditional asymptotic approximation of the MHD pipe flow [8], the Roberts layers are not taken into account: the velocity profiles in the core and Hartmann layers are matched and the core velocity is determined by taking into account the pipe's electrical boundary condition. The resulting expressions for the velocity along the x- and y-axis, normalised with the velocity at the center of the pipe $u_c = u(x = 0, y = 0) = -\frac{(1+c)L^2\partial_z p}{\rho\nu(1+c\,Ha)Ha}$

(with u_c in terms of non-rescaled variables), read [8]:

$$\frac{u(x, y = 0)}{u_c} = \frac{(1 + cHa)\sqrt{1 - x^2}}{1 + cHa\sqrt{1 - x^2}} \tag{7}$$

$$\frac{u(x = 0, y)}{u_c} = 1 - \exp\left(Ha(|y| - 1)\right) \tag{8}$$

We recall the important difference between the insulating pipe and the conducting pipe, that is, u_c scales as Ha^{-1} for $c = 0$ and as Ha^{-2} for $c = \infty$.

4 Numerical method

We use a node-based, unstructured finite-volume method to solve the set of equations (1),(4) and (5). On regular grids, the spatial discretization is second order accurate. On unstructured grids, like ours, it is first order accurate in regions of space where the grid is skewed or stretched. One key feature of our code, is the use of a charge-conserving algorithm, which has been shown to be crucial at high Hartmann numbers [12], [13]. This means that the currents at the grid nodes are interpolated from the current fluxes at the faces using the following identity: $\mathbf{j} = \nabla \cdot (\mathbf{j}\mathbf{r})$, with $\mathbf{r}$ the position vector (see 10 for the discrete form of this expression). This is very desirable, since it implies that the numerical computation mimics the physical property that the integration of the Lorentz force (or current) over the computation domain reduces to a boundary term. As such, no spurious net Lorentz force is introduced by discretisation errors.

To obtain the steady profile, we start from the arbitrary initial fields $u \equiv 0, \phi \equiv 0$, and advance them in time according to equations (1),(4) and (5) until convergence is reached. For the Lorentz force term, we prefer an explicit Euler scheme because it decouples the Poisson equation for the potential from the velocity advancement. The viscous term is discretized with an implicit Euler scheme for stability reasons. We can summarize the procedure to advance the fields one step in time with the following four-step algorithm:

1. Compute the velocity at time $n+1$ from that at time n using the simplified Navier-Stokes equations:

$$\frac{u^{n+1} - u^n}{\Delta t} = \frac{1}{Ha^2}\nabla^2 u^{n+1} - \partial_z p + (\mathbf{j}^n \times \mathbf{1_y})_z \tag{9}$$

2. Find the potential at time $n + 1$ from the Poisson equation (4)

$$\nabla^2 \phi^{n+1} = \nabla \cdot \left(\mathbf{u}^{n+1} \times \mathbf{1_y}\right) \tag{10}$$

3. Calculate current fluxes J_f^{n+1} through the nodal volume faces such that the discrete divergence of the current is of the order of machine accuracy: $\sum_{faces} J_f^{n+1} A_f \approx 0$, where the summation is taken over all the faces of one nodal volume and where A_f represents the area of face f.

4. Obtain the nodal current $\mathbf{j}^{n+1}$ from the aforementioned current-conservative algorithm:

$$\mathbf{j}_{node}^{n+1} = V_{node}^{-1} \sum_{faces} J_f^{n+1} A_f \mathbf{r}_f \qquad (11)$$

with V_{node} the volume of the control volume associated with the node. This nodal current can then be injected in expression (9) to calculate the velocity u^{n+2} from the fields at instant $n + 1$.

We solve the discrete equations on two-dimensional meshes which consist of quadrilateral elements. Close to the wall, we use a stretching function in order to properly resolve the Hartmann layers and other wall effects. At sufficiently high resolution, we have checked that the solutions become mesh-independent. The results that we show in this work, are the ones obtained on the most fine meshes, containing 86450 nodes ($Ha < 400$) or 342000 nodes ($Ha \geq 400$).

5 Results and discussion

Figure 2 shows numerical and asymptotical solutions for a flow at $Ha = 2000$, for both a perfectly insulating and perfectly conducting pipe. We consider cuts of the velocity profile along the two main axes. For the insulating case ($c = 0$), we observe a quasi-perfect agreement between our numerical method and the asymptotic solution. In the conducting case ($c = \infty$), the agreement is again excellent along the y-axis (in the direction of the magnetic field), whereas there is a significant discrepancy in the results along the x-axis: small zones of overspeed appear in the numerical solution, whereas the asymptotic approximation predicts a flat profile.

In figure 3, we focus on the region between $x = 0.8$ and $x = 1.0$ for a flow at the same Hartmann number ($Ha = 2000$), and consider four different values of the wall conductance. The figure shows that the jets appear gradually near the wall, with at first the emergence of a plateau, followed by the formation of small side bumps with velocities below the core velocity, which grow eventually into zones of overspeed.

We choose to define the wall conductance parameter c_{crit} that marks the emergence of the overspeed regions as the minimum c for which the velocity profile has a local maximum at positions different from the pipe axis. This yields a curve in the (Ha, c)-plane that is displayed in figure 4. The results can be summarized as follows:

– The lowest Hartmann number for which we observe a velocity overspeed, is $Ha = 12$. Overspeed regions were observed earlier in this Hartmann range ($Ha = 18$) by Samad [6].
– The curve goes through a local minimum at $Ha = 35$ and a local maximum at $Ha = 41$. For lower values of the Hartmann number, the curve has a steep descent; at higher Hartmann numbers, c_{crit} follows a power-law like behaviour.
– We can fit the results for $Ha \geq 250$ with the relationship $c_{crit} \propto Ha^{-2/3}$.
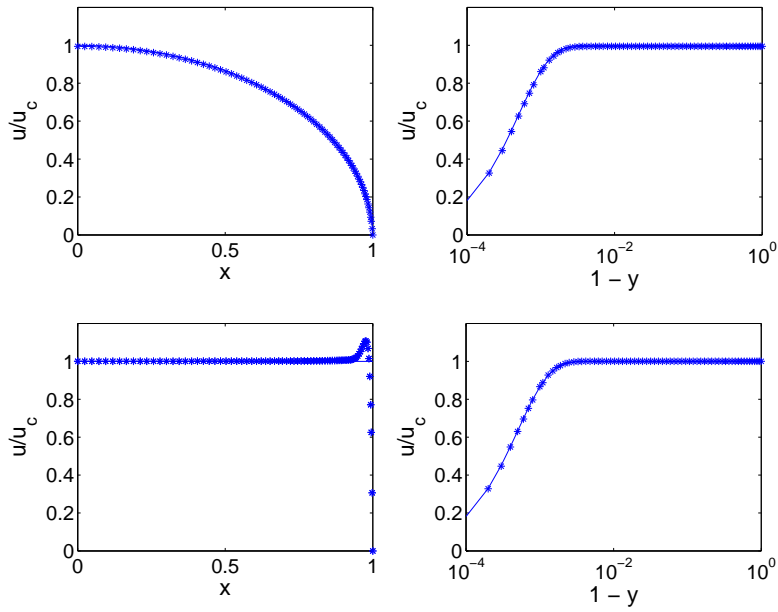
Fig. 2 Normalised velocity profiles for the laminar flow at $Ha = 2000$ in a pipe with perfectly insulating (top) and perfectly conducting (bottom) walls along the axes perpendicular (left) and parallel (right) to the field. Comparison between the asymptotic approximations (solid line) and the numerical solution ($\times$).
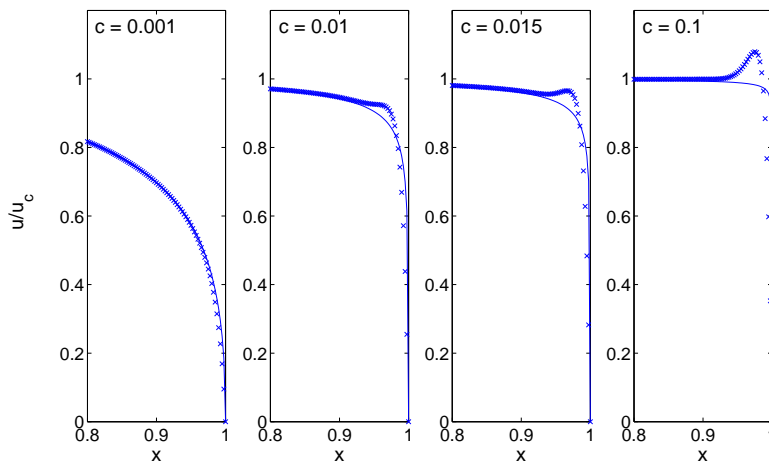

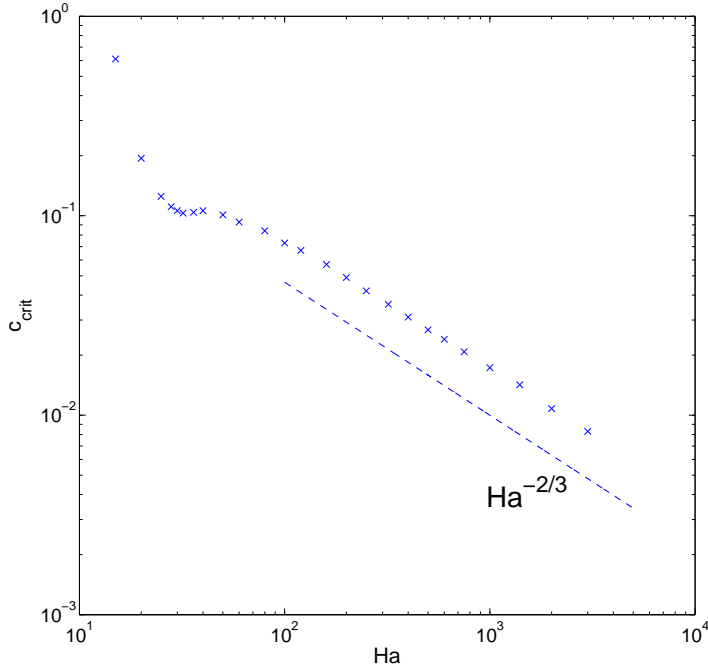**Fig. 3** Emergence of the overspeed zones with increasing c, illustrated for a flow at $Ha=2000$. Asymptotic approximations (solid line) and numerical simulations ($\times$).

Fig. 4 Limiting values c_{crit} ($\times$) for the emergence of overspeed regions as a function of the Hartmann number and fitted power-law like behaviour ($--$).

We define the relative amplitude α of the overspeed region as the ratio between the local maximum and core velocity. Figure 5 displays the value of α as function of the Hartmann number for different values of the wall conductance. For $c = \infty$ and $c = 1.0$ and in the limit of $Ha \rightarrow \infty$, α clearly converges to a value slightly above 11 %. For $c = 0.1$, the values of the Hartmann number considered are not high enough to observe the same asymptote. However, it seems reasonable to conjecture that α scales like $O(Ha^0)$, provided that c and Ha are sufficiently high.

To find the proper scaling for the width of the overspeed regions along the x-axis, we introduce the coordinate $\xi = 1-x$, and investigate how the position of the velocity maximum ξ_{max} scales with the Hartmann number. From the data in the left-hand side of figure 6, we conclude that, for Ha between 250 and 3000, ξ_{max} scales as $Ha^{-2/3}$ (for $c = 0.1$, this scaling is probably reached only at the highest values of the Hartmann numbers considered). This scaling matches the $Ha^{-2/3}$ scaling of the zone where the asymptotic approximation breaks down, obtained by Roberts in his analysis for the perfectly insulating pipe [14].
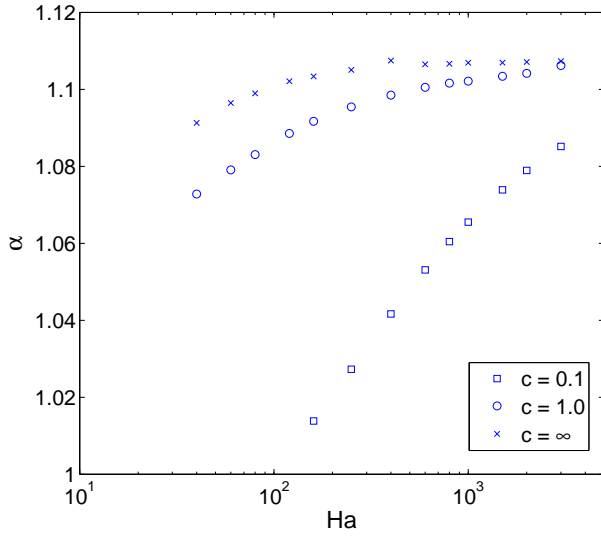
Fig. 5 Relative amplitude of the overspeed zones as a function of Ha for different values of c.

In the same work, Roberts also derived for $c = 0$ that these regions are responsible for a contribution of $O(Ha^{-7/3})$ to the asymptotic expression for the flow rate.

In the right-hand side of figure 6, we show the relative flow rate deficit $\Delta Q = (Q_{numerical} - Q_{asymptotic})/Q_{asmptotic}$ as a function of the Hartmann number. The asymptotic flow rate $Q_{asymptotic}$ does not contain Hartmann or side layer correction terms, and is given by [8]:

$$Q_{asymptotic} = 4u_c(1 + c\,Ha)\left(\frac{\pi}{4c\,Ha} - \frac{1}{(c\,Ha)^2} + \frac{\pi}{2(c\,Ha)^3}\right.$$
$$\left. - \frac{2}{(c\,Ha)^3}\frac{\operatorname{arctanh}\left(\sqrt{\frac{c\,Ha-1}{c\,Ha+1}}\right)}{\sqrt{(c\,Ha)^2 - 1}}\right) \quad (12)$$

Figure 6 (r.h.s) shows us thus that the combined Hartmann and side layer correction term scales as Ha^{-1}. It is however not straightforward to consider the contribution of the side jets alone. Nevertheless, figure 7 gives an indication of how small the side layer correction term might be; the numerical profile along the x-axis is partially below and partially above the asymptotic profile. For the values of the Hartmann number and coductance ratio considered, these positive and negative corrections to the flow rate always cancel each other nearly perfectly; hence, it is very likely that the overspeed regions induce a flow rate correction that is much smaller than one would intuitively expect.
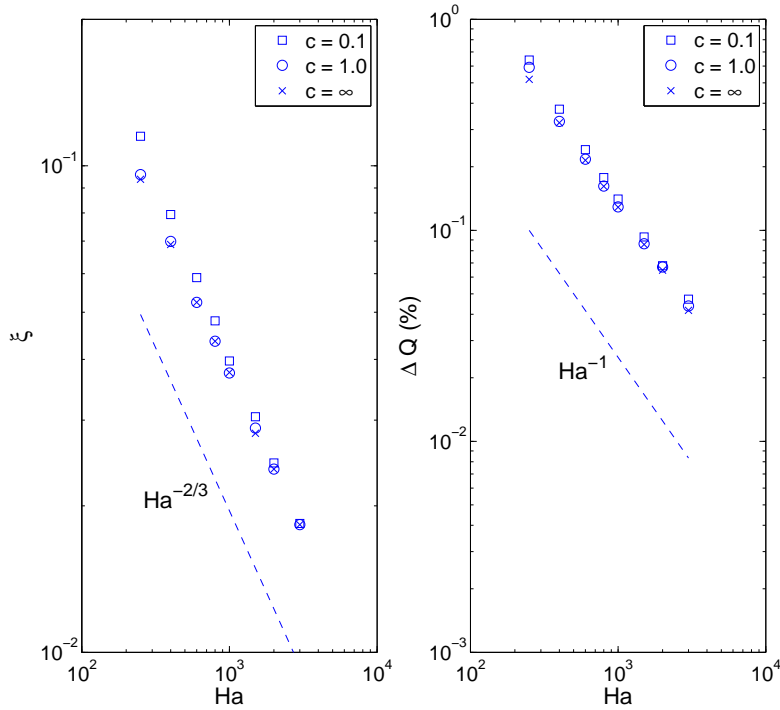
Fig. 6 Scaling laws in the conducting pipe: Position of the velocity maximum ξ_{max}(l.h.s.) and flow rate deficit ΔQ (r.h.s.) as function of the Hartmann number for three different values of the wall conductance.

6 Conclusion

By means of numerical simulations without model, based on a conservative formulation for the current, we were able to investigate in detail the laminar magnetohydrodynamic pipe flow in a wide parameter range. We observe overspeed regions at sufficiently high values of the Hartmann number and the wall conductance ratio. These overspeed regions do not disappear as $Ha \to \infty$ but are of order $O(Ha^0)$ compared to the core velocity. This behavior is similar to what was observed in [15] in the case of the perfectly conducting duct flow. We also characterize the lateral extent of the overspeed zones and show that they are fine enough to fit in a region that the earlier asymptotic expression of [8] cannot predict.
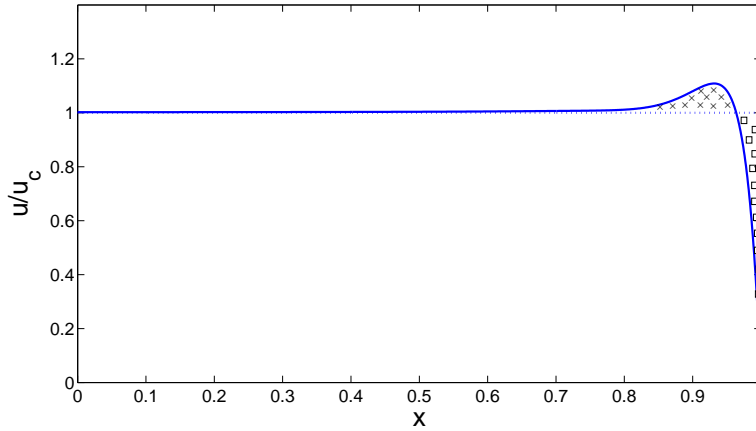
Fig. 7 Contribution of the overspeed regions to the flow rate for a perfectly conducting pipe at $Ha = 400$. Positive ($\times$) and negative ($\square$) corrections of the numerical solution (solid line) to the asymptotic theory (dashed line).

References

1. Shercliff, A., 1956. "The flow of conducting fluids in circular pipes under transverse magnetic fields". *J. Fluid Mech.,* **1**, pp. 644–666.
2. Hartmann, J., 1937. "Hg-dynamics I. Theory of the laminar flow of an electrically conductive liquid in a homogeneous magnetic field". *K. Dan. Vidensk. Selsk. Mat. Fys. Medd.,* **XV**(6), pp. 1–28.
3. Hartmann, J., and Lazarus, F., 1937. "Hg-dynamics II. Experimental investigations on the flow of mercury in a homogeneous magnetic field". *K. Dan. Vidensk. Selsk. Mat. Fys. Medd.,* **XV**(7), pp. 1–45.
4. Gold, R. R., 1962. "Magnetohydrodynamic pipe flow. part 1". *J. Fluid Mech.,* **13**, pp. 505–512.
5. Ihara, S., Kiyohiro, T., and Matsushima, A., 1967. "The flow of conducting fluids in circular pipes with finite conductivity under uniform transverse magnetic fields". *J. Appl. Mech,* **34**(1), pp. 29–36.
6. Samad, S., 1981. "The flow of conducting fluids through circular pipes having finite conductivity and finite thickness under uniform transverse magnetic fields". *Int. J. Eng. Sci.,* **19**, pp. 1221–1232.
7. Shercliff, A., 1962. "Magnetohydrodynamic pipe flow. Part 2. High Hartmann number.". *J. Fluid Mech.,* **13**, pp. 513–518.

8. Chang, C., and Lundgren, S., 1961. "Duct flow in magnetohydrodynamics". *ZAMP,* **XII**, pp. 100–114.

9. Mistrangelo, C., 2005. "Three-dimensional MHD flow in sudden expansions". PhD thesis, Fakültat für Maschinenbau, Universität Karlsruhe.

10. Roberts, P. H., 1967. *An Introduction to Magnetohydrodynamics.* American Elsevier Publishing Company, Inc. New York.

11. Walker, J. S., 1981. "Magnetohydrodynamic flows in rectangular ducts with thin conducting walls". *Journal de Mécanique,* **20**(1), pp. 79–112.

12. Ni, M.-J., Munipalli, R., Morley, N. B., Huang, P., and Abdou, M. A., 2007. "A current density conservative scheme for incompressible mhd flows at a low magnetic reynolds number. part I: On rectangular collocated grid system". *J. Comput. Phys.,* **221**(1), pp. 174–204.

13. Ni, M. J., Munipalli, R., Huang, P., Morley, N. B., and Abdou, M. A., 2007. "A current density conservative scheme for incompressible mhd flows at a low magnetic reynolds number. part II: On an arbitrary collocated mesh". *J. Comput. Phys.,* **227**(1), pp. 205–228.

14. Roberts, P. H., 1967. "Singularities of hartmann layers". *Proc. Roy. Soc. A.,* **300**, pp. 94–107.

15. Hunt, J. C. R., 1965. "Magnetohydrodynamic flow in rectangular ducts". *J. Fluid Mech.,* **21**(4), pp. 577–590.